UCRL-JC-132943
Preprint

High-Performance Computational and Geostatistical Experiments for Testing the Capabilities of 3-D Electrical Resistance Tomography

S. Carle, A. Ramirez, W. Daily, R. Newmark and A. Tompson

This paper was prepared for submittal to
The 12th Annual Symposium on the Application of Geophysics to Environmental and Engineering Problems (SAGEEP)
Oakland, CA
March 14-18, 1999

January 19, 1999

Lawrence Livermore National Laboratory

DISCLAIMER

HIGH-PERFORMANCE COMPUTATIONAL AND GEOSTATISTICAL EXPERIMENTS FOR TESTING THE CAPABILITIES OF 3-D ELECTRICAL RESISTANCE TOMOGRAPHY

Steven Carle, Abelardo Ramirez, William Daily, Robin Newmark, and Andrew Tompson

Lawrence Livermore National Laboratory, L-206, POB 808, Livermore, CA 94551

Abstract

This project explores the feasibility of combining geologic insight, geostatistics, and high-performance computing to analyze the capabilities of 3-D electrical resistance tomography (ERT). Geostatistical methods are used to characterize the spatial variability of geologic facies that control subsurface variability of permeability and electrical resistivity. Synthetic ERT data sets are generated from geostatistical realizations of alluvial facies architecture. The synthetic data sets enable comparison of the "truth" to inversion results, quantification of the ability to detect particular facies at particular locations, and sensitivity studies on inversion parameters.

INTRODUCTION

A geophysical tomograph does not directly convert into a permeability field, not only because the geophysical property does not directly correlate to permeability, but because the resolution of a tomograph varies with location. The resolution may be inadequate for characterization of flow and transport processes, so that means for interpreting the ERT inversion in a hydrogeologic context are needed. The tomographic inversion is nonunique, that is, different parameters can yield similar fit to the data. The degree to which a tomograph will provide additional insight is difficult to quantify and depends on the survey configuration, the characteristics of the subsurface heterogeneity, and prior knowledge of site geology.

This study examines the resolution and parameter sensitivity of electrical resistance tomography (ERT) using synthetic data sets generated from a realistic representation of a geologic system. ERT images subsurface electrical resistivity structure by mathematical inversion of voltage measurements induced by current applied to an array of electrode pairs. The inversion is mathematically nonunique and sensitive to data noise and the initial "roughness coefficient," which controls the degree of smoothness in the inversion (LaBrecque et al., 1996). ERT is a promising tool for hydrogeologic characterization because in freshwater alluvial systems electrical resistivity correlates with clay content (Waxman and Thomas, 1974), which strongly influences permeability, and resistivity contrasts are typically much larger that seismic velocity contrasts.

From a geologic point of view, the origin of variations in permeability may be very clearly related to geologic processes, to the extent that a geologist can predict realistic (but not deterministic) patterns of spatial variability. However, conventional geologic interpretation by means of cross-sections or fence diagrams would require painstaking efforts to develop multiple, geologically plausible 3-D models. Alternatively, geostatistical methods can quantitatively generate three-dimensional (3-D) "realizations" of geologic architecture.

This project employs geostatistical methods to gain insight into the capabilities and limitations of 3-D ERT inversion. One difficulty with evaluating the accuracy of an ERT tomograph is that the"truth," the true spatial distribution of electrical resistivity, is not known. Granted, synthetic data sets have been inverted to illustrate the capabilities of ERT, but these examples are usually too simplistic and not relevant to site-specific geologic heterogeneity.

Alternatively, this project performs inversions on synthetic ERT data sets derived from 3-D resistivity distributions based on geostatistical realizations consistent with geologic architecture observed in the alluvial fans underlying the Lawrence Livermore National Laboratory (LLNL). The synthetic ERT data sets were generated using the high-performance flow finite-difference modeling code ParFlow developed at LLNL (Ashby, 1996; Tompson et al., 1998). The synthetic ERT data sets not only enable comparison of inversion results to the "truth," but yield insights into the sensitivity of inversion parameters. The geostatistical methods employed enable a simplified quantification of inversion results in terms of the probability of locating a particular facies at a particular location.

The experimental procedure consists of the following steps:

1. developing a realistic geologic facies model and translating that into geostatistical parameters,
2. generating multiple geostatistical realizations conditioned to borehole facies,
3. assigning plausible resistivity values to each facies based on previous ERT field work,
4. generating synthetic ERT data sets using ParFlow,
5. inverting the synthetic data sets using the program MultiBH,
6. quantifying the degree to which ERT improves the subsurface characterization, and
7. performing sensitivity analyses on inversion parameters.

GEOLOGIC INTERPRETATION

In the unconsolidated alluvial sediments underlying LLNL, spatial variation of permeability at the scale (~0.3 m vertical, ~3 m lateral) relevant to intra-well flow and transport typically spans over five orders of magnitude and is primarily related to the spatial distribution of geologic facies. The term "facies" refers to rock categories with distinctive and identifiable characteristics, which are related to textural and depositional properties for the LLNL alluvial system. These facies are recognized in core samples and excavated exposures as follows:

Facies	**Proportion**	**Description**
f1 : channel	12%	well sorted sand with gravelly lag deposits, fining upward
f2 : stream flood	8%	poorly sorted gravel supported by a silty/sandy matrix
f3 : bar/levee	21%	silty fine sand
f4 : flood plain	59%	silt and clay, some indurated and with caliche

Our geologic interpretation concludes that high permeability zones consist of an interconnected network of *channel* and *stream flood* deposits. These high permeability zones correlate to relatively high electrical resistivity zones.

GEOSTATISTICAL ANALYSIS

A categorical (indicator) geostatistical approach was used to quantify spatial variability of the geologic facies. Using core data form several boreholes at LLNL, a matrix of transition probabilities (Figure 1) for the vertical direction (z) was obtained. The *transition probability* matrix entry $t_{jk}(h_z)$ as a function of separation vector or "lag" h_z is simply defined by

$$t_{jk}(h_z) = \Pr\{k \text{ occurs at } \mathbf{x}+h_z \mid j \text{ occurs at } \mathbf{x}\}$$

where $\mathbf{x}$ is a spatial location, and j and k denote "facies j" and "facies k," respectively.

The solid line indicates a continuous-lag Markov chain or"matrix exponential" model defined by

$$t_{jk}(h_z) = \exp\left[\mathbf{R}_z h_z\right]$$

where $\mathbf{R}_z$ represents the vertical *transition rate* matrix (Carle and Fogg, 1997). Transition rate matrix entries correspond to slopes at the lag origin, which indicate *mean length* or "thickness" for the diagonal entries and juxtapositional tendencies for the off-diagonal entries. The "sills" or $t_{jk}(h_z \to \infty)$ indicate category proportions p_k of the column entries.

Borehole spacing is usually inadequate for direct measurement of lateral spatial variability. However, considering that the parameters of the Markov chain consist of the geologically interpretable concepts of proportions, mean length, and juxtapositional tendencies, the transition probability/Markov geostatistical approach provides a framework for developing geologically plausible models of lateral spatial variability (Carle, 1998; Carle et al., 1998). A 3-D Markov chain model was used to generate multiple stochastic realizations of facies architecture conditional to the borehole data with discretization of $\Delta x = 1.2$ m, $\Delta y = 1.2$ m, $\Delta z = 0.3$. Figure 2 shows two realizations, where the exposed inner block is conditioned by borehole data at the four corners and is the region to which the ERT inversion is applied. The full blocks are used in generation of the synthetic ERT data.

SYNTHETIC ERT DATA SETS

Previous 2-D ERT surveys at LLNL showed correlation between electrical resistivity and geologic facies, with about two orders of magnitude variation in resistivity primarily attributed to variation in clay content (Ramirez et al., 1993). Accordingly, the facies $f1, f2, f3$, and $f4$ were assigned resistivities of 100, 20, 5, and 1 ohm-m, respectively, for generation of the synthetic ERT data sets.

The synthetic ERT data were generated using ParFlow, a high-performance parallel finite difference groundwater flow modeling code developed by LLNL (Ashby, 1996; Tompson et al., 1998). The flow simulation capabilities of ParFlow are intriguing in that very large problems can be rapidly solved with robust convergence. Considering that flow of electrical current in the subsurface is analogous to the flow of groundwater, this study adapted ParFlow for simulation of voltage response in application of ERT. ParFlow employs a Tool Command Language script interface that is programmable (Welch, 1997), so that the ParFlow runs and output could be customized to mimic an ERT survey. The finite difference grid was refined with respect to the geostatistical grid to $\Delta x = 0.4$ m, $\Delta y = 0.4$ m, $\Delta z = 0.3$ m to ensure accuracy of the flow solutions.

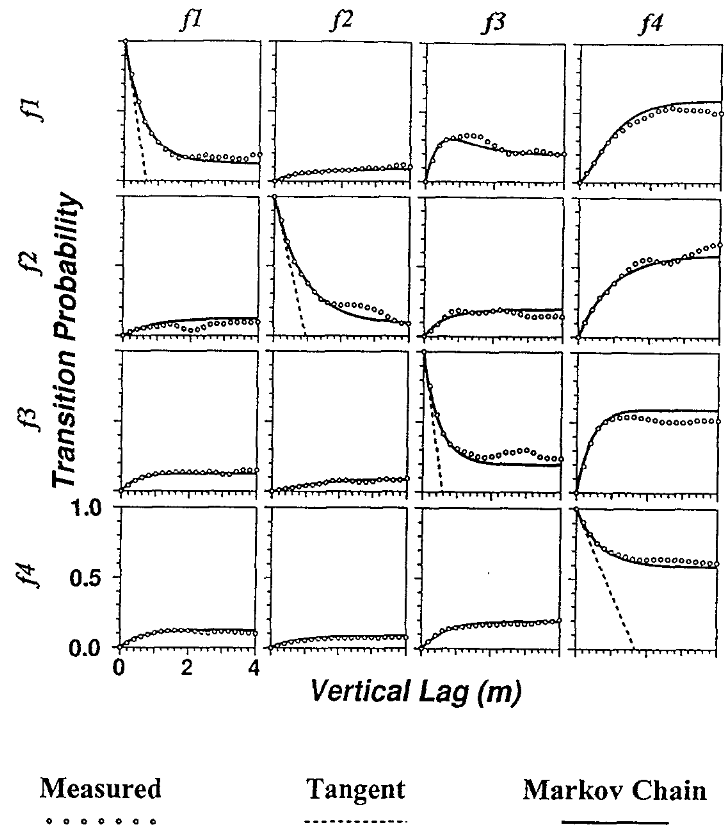

Figure 1: Matrix of transition probabilities between facies as a function of vertical lag. The intercept of the tangent at the lag axis corresponds to mean length. The model curves converge at the column facies proportions.

ParFlow was used to generate 100 synthetic 3-D ERT data sets, based on four boreholes spaced at 14.4 m with 15 electrodes spaced at 1.8 m. Each data set required 60 ParFlow runs on a grid of 800,000+ cells. The synthetic ERT data permit comparison of ERT inversions to the"truth," facilitating sensitivity studies and enabling quantification of the ability to resolve intra-well heterogeneity. Figures 3 and 4 show close-up comparisons of realizations #11 and #13 and corresponding ERT inversions of the synthetic data.

QUANTIFICATION OF PREDICTIVE CAPABILITIES

Resolution of the ERT inversion generally deteriorates away from the borehole, such that the tomograph yields a more smoothed image of resistivity structure at locations more distant from the boreholes. Obviously, one cannot expect to directly convert resistivity values to permeability values. Resolution can be mathematically quantified for each of the cells of the ERT inversion (Vasco et al., 1997). However, the more practical issue is how does resolution affect predictive capabilities, that is, how can one use the ERT tomograph for hydrogeologic interpretation in light of the

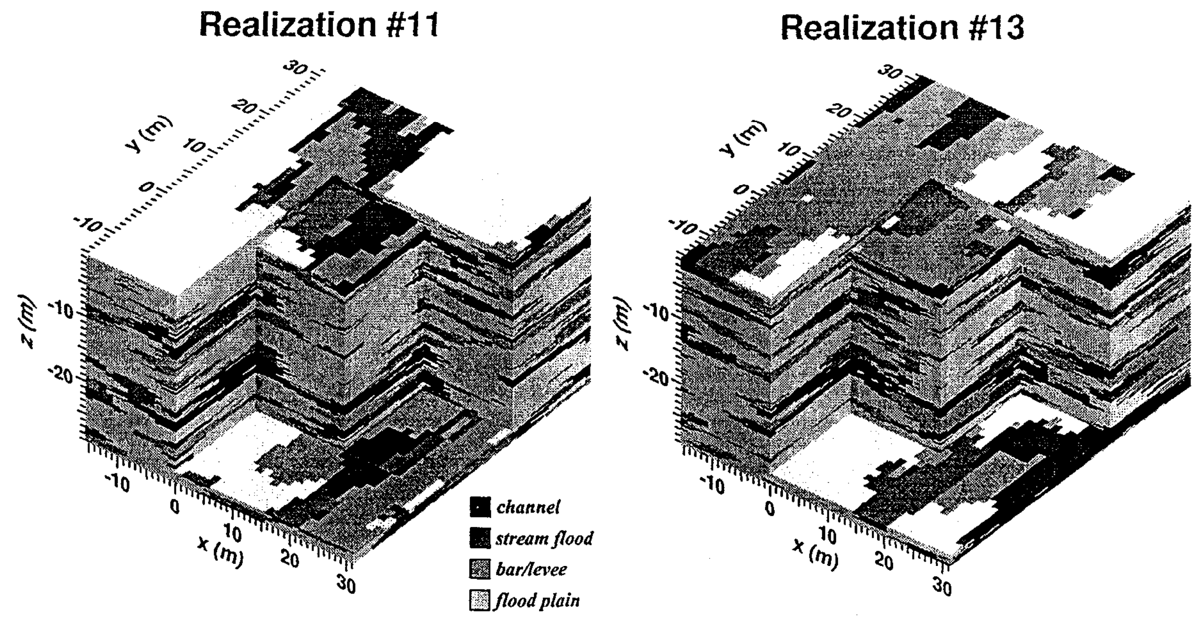

Figure 2: Two stochastic realizations generated from a 3-D Markov chain model.

variable resolution? For example, if characterization of hydraulic connectivity is of concern, how can the ERT inversion be quantitatively evaluated in terms of determining whether permeable units are continuous between boreholes?

The synthetic data sets offer an opportunity to evaluate the predictive capabilities of ERT. In a direct interpretation, one would attempt to convert the resistivity values of the ERT inversion into permeability. In this study, the interpretation is posed with respect to resistivity *categories* and facies; given that the ERT inversion indicates a particular resistivity quantile (category) at a particular location, the probability that a particular facies occurs at that location is predicted.

Let the indicator value $I_j(\mathbf{x}, d)$ define whether an ERT inversion resistivity $\rho(\mathbf{x})$ falls into the quantile q_k defined by resistivity cutoff values $c_j(d)$ as a function of radial distance d from the borehole:

$$I_j(\mathbf{x}, d) = \begin{cases} 1, & \text{if } \rho(\mathbf{x}) \in q_j \\ 0, & \text{otherwise} \end{cases}$$

where q_j is defined by $c_j(d) \leq \rho(\mathbf{x}) < c_{j-1}(d)$ with $c_{j-1}(d) > c_j(d) > c_{j+1}(d)$. Let another indicator value $J_k(\mathbf{x})$ define the presence or absence of facies k at location $\mathbf{x}$:

$$J_k(\mathbf{x}) = \begin{cases} 1, & \text{if facies } k \text{ occurs at } \mathbf{x} \\ 0, & \text{otherwise} \end{cases}$$

Then, the probability $\Pr\{k \text{ at } \mathbf{x} \mid \rho(\mathbf{x})\}$ that facies k occurs at $\mathbf{x}$ given the ERT inversion resistivity

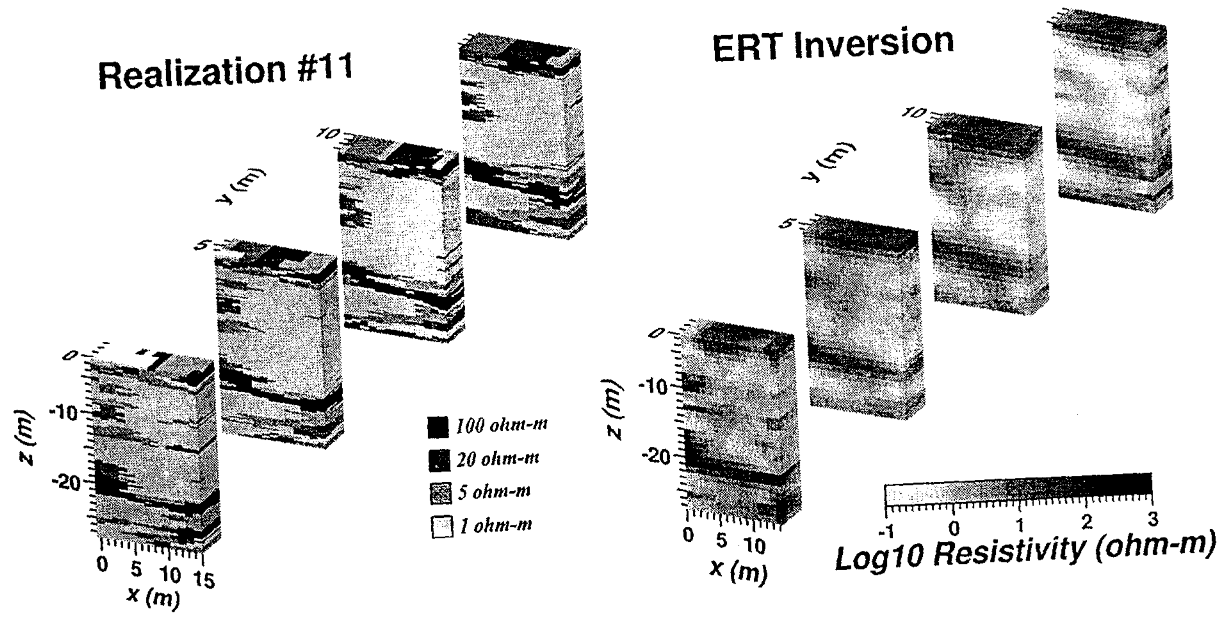

Figure 3: Comparison of "truth," realization #11, to an ERT inversion. Inverted region (inner block from Figure 2) is exploded to reveal internal 3-D structure.

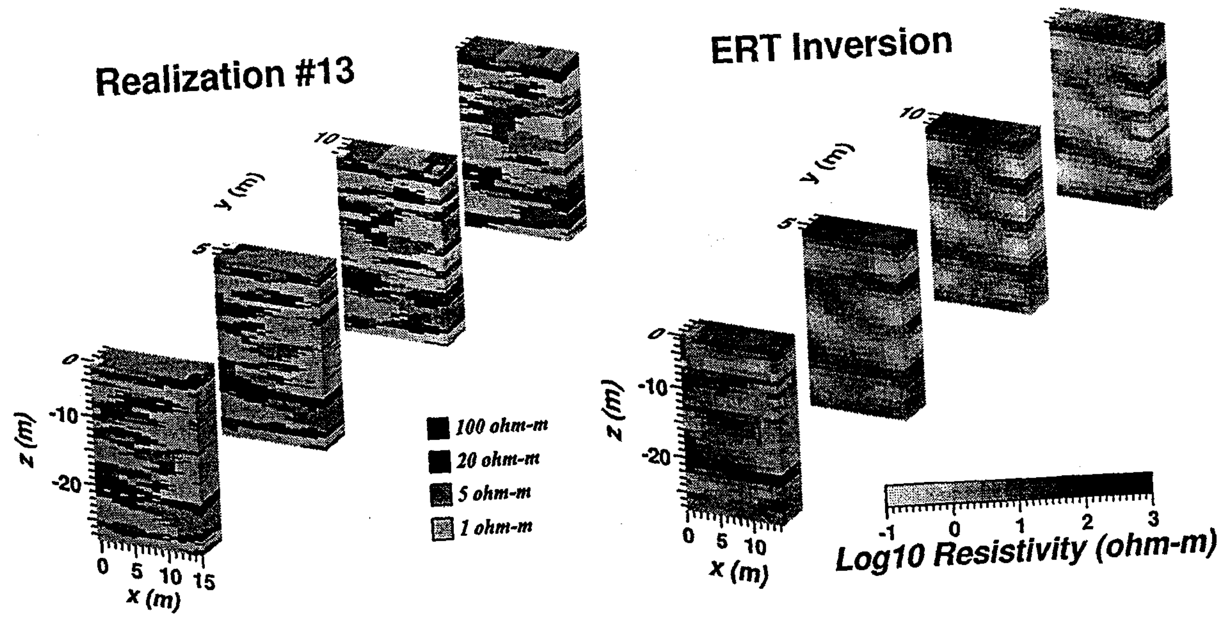

Figure 4: Comparison of "truth," realization #13, to an ERT inversion. Inverted region (inner block from Figure 2) is exploded to reveal internal 3-D structure.

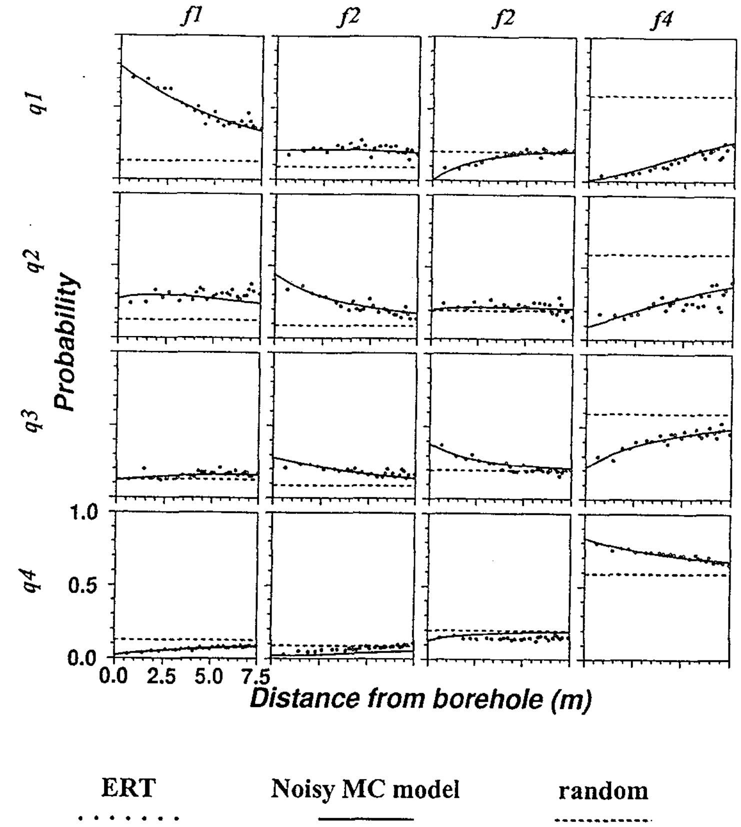

Figure 5: Matrix showing $\mathbf{P}(d)$, the probability of facies k occuring given resistivity quantile j as a function of distance d from borehole, as averaged from 18 realizations and ERT inversions.

$\rho(\mathbf{x})$ can be estimated from the conditional probability $P_{jk}(d)$ defined as:

$$\Pr\{k \text{ at } \mathbf{x} \mid \rho(\mathbf{x})\} \approx P_{jk}(d) = \frac{E\{I_j(\mathbf{x}, d)\ J_k(\mathbf{x})\}}{E\{I_j(\mathbf{x}, d)\}}$$

The entries $P_{jk}(d)$ in the matrix $\mathbf{P}(d)$ are calibrated from the values of $J_k(\mathbf{x})$ in the realizations and the values of $I_j(\mathbf{x}, d)$ in the ERT inversions. Figure 5 shows a plot of $\mathbf{P}(d)$ calibrated from 18 realizations and inversions. A "noisy" Markov chain model was fitted to the data by the formula

$$\mathbf{P}(d) = \mathbf{P}(0) \exp\left[\mathbf{R}_p d\right]$$

where $\mathbf{R}_p$ is a rate matrix. The resistivity quantiles are divided according to the facies proportions such that $E\{I_j(\mathbf{x}, d)\} = p_j$. For example, the $P_{11}(d)$ term in the upper left corner of the matrix represents the probability that *channel* $(f1)$ occurs given that the ERT inversion resistivity value falls within in the highest quantile $q1$ defined such that $E\{I_1(\mathbf{x}, d)\} = 0.12$, the proportion of *channel* facies. $P_{11}(d)$ declines with distance from the borehole because of declining resolution.

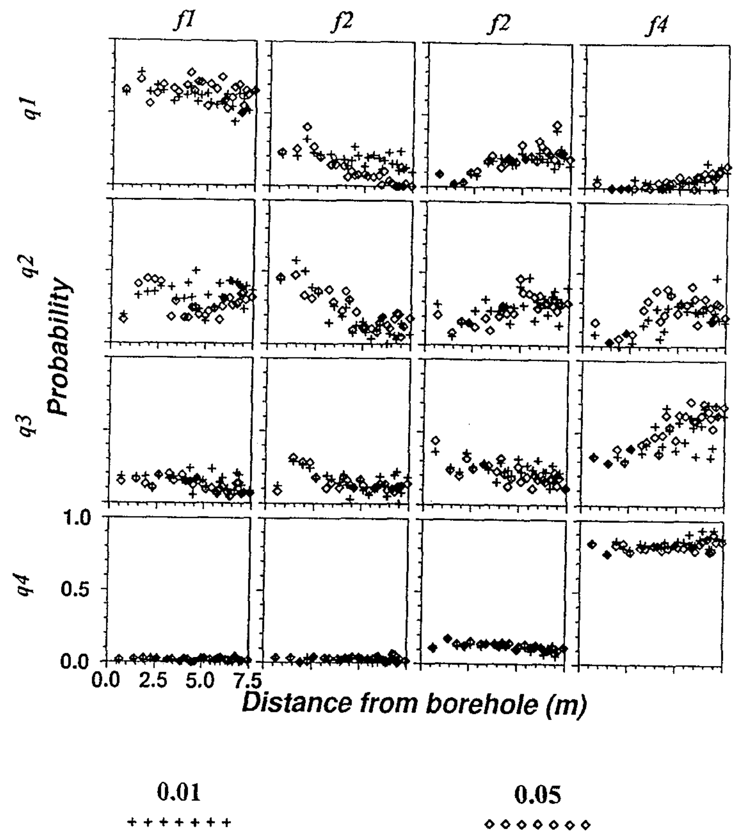

Figure 6: Sensitivity study comparing $\mathbf{P}(d)$ from inversion results for two different values, 0.01 and 0.05, of the initial roughness coefficient used in the ERT inversion.

If resolution and accuracy of the ERT inversion were perfect, then $P_{11}(d) = 1$; if the correlation between the ERT inversion and the realization were completely random, then $P_{11}(d) = 0.12$. In this example, $0.12 < P_{11}(d) < 1$, indicating the degree to which the ERT inversion improves prediction of the location of the high permeability *channel* facies as a function of distance from the borehole.

The off-diagonal terms indicate the probability of misinterpreting a particular facies. For example, $P_{14}(d)$ indicates the probability that *flood plain* (lowest resistivity facies) occurs given that the highest quantile ERT inversion resistivity occurs at x. If the resolution and accuracy of ERT inversion were perfect, then $\mathbf{P}(d)$ would correspond to an identity matrix for all d; if the correlation between the ERT inversion and the realization were completely random, then $P_{jk}(d) = q_k$ where q_k are the quantile proportions. In this example, the q_k were chosen to correspond to the facies proportions p_k.

SENSITIVITY STUDIES

Two crucial parameters in the ERT inversion algorithm are data noise level and the "roughness" coefficient (LaBrecque et al., 1996). The data noise level can be estimated by repeated and reciprocal measurements. However, experience generally dictates selection of the initial value of the roughness coefficient. The roughness coefficient controls the degree of weighting in the objective function devoted to minimization of roughness of the resistivity field. If a roughness coefficient of zero is assumed, the inversion process would likely produce a tomograph that matches the data very precisely, but with an unrealistically high degree of spatial variability of resistivity. If the roughness coefficient is too high, the inversion may not converge, or the tomograph may be unrealistically smooth. The roughness coefficient is adjusted throughout the ERT inversion, however, the final inversion result is sensitive to the initial value.

Figure 6 shows a comparison of $\mathrm{P}(d)$ for two different values of the initial value of the roughness coefficient, 0.01 and 0.05, applied to the same ERT data set. The $\mathrm{P}(d)$ values, although different, indicate that the resulting inversions have similar accuracy.

CONCLUSIONS

ERT provides a promising tool for characterization of 3-D intra-well heterogeneity. 3-D inversions of synthetic ERT data consistently detected major high permeability zones, locations of which are uncertain for the degree of spatial variability observed in the field. The practice of generating and inverting realistic synthetic ERT data sets provides means for conducting feasibility and sensitivity studies and is made possible by emerging geostatistical methods and numerical flow modeling capabilities. An important result is to *quantify* the probability that a particular facies will occur at a particular location based on the ERT inversion. The geostatistical parameters can be tuned to site specific conditions, so that the method described in this paper may be applied to different sites. Practical implementation of the method requires only an accurate conceptual model of the geologic variability, assuming that the geologic variability can be described by the geostatistical parameters and that the resistivity variations are associated with the geology. The method would be a useful tool for diagnosing the effectiveness of implementing an ERT survey *before* deployment of the field work. Future work will use ERT inversions as soft conditioning to constrain the geostatistical realizations, with the goal of finding ERT inversions that are geologically plausible.

ACKNOWLEDGMENTS

This work was performed under the auspices of the U.S. Department of Energy by Lawrence Livermore National Laboratory under contract No. W-7405-Eng-48.

References

Ashby, S. F., 1996, ParFlow home page: http:/www.llnl.gov/CASC/ParFlow/

Carle, S. F., and Fogg, G. E., Modeling spatial variability with one- and multidimensional continuous-lag Markov chains: Mathematical Geology, v. 29, p. 891-918.

Carle, S.F., Labolle, E. M., Weissmann, G. S., Van Brocklin, D. V., and Fogg, G. E., 1998, Conditional simulation of hydrofacies architecture, a transition probability/Markov approach: In Fraser, G. S., and Davis, J. M., Hydrogeologic Models of Sedimentary Aquifers, Concepts in Hydrogeology and Environmental Geology No. 1, SEPM Special Publication, p. 147-170.

Carle, 1998, T-PROGS, Transition Probability Geostatistical Software, version 2.0: available on request by e-mail to carle1@llnl.gov or gefogg@ucdavis.edu .

LaBrecque, D. J, Milleto, M., Daily, W., Ramirez, A., and Owen, E., 1996, The effects of noise on Occam's inversion of resistivity tomography data: Geophysics, v. 61, n. 2, p. 538-548.

Ramirez, A., Daily, W., LaBrecque, D. J., Owen, E., and Chestnut, D., 1993, Monitoring an underground steam injection process using electrical resistance tomography: Water Resources Research, v. 29, n. 1, p. 73-87.

Tompson, A. F. B., Falgout, R. D., Smith, S. G., Bosl, W. J., and Ashby, S. F., 1998, Analysis of subsurface contaminant migration and remediation using high performance computing: Advances in Water Resources, v. 22, n. 3, p. 203-221.

Vasco, D. W., Datta Gupta, A., Long, J. C. S., 1997, Resolution and uncertainty in hydrologic characterization: Water Resources Research, v. 33, n. 3, p. 379-397.

Waxman, M. H., and Thomas, E. C., 1974, Electrical conductivities in shaly sands - I. The relation between hydrocarbon saturation and resistivity index; II. The temperature coefficient of electrical conductivity: Journel of Petroleum Technology, Transactions AIME, 257, (Feb. 1974) p. 213-225.

Welch, B. B., 1997, Practical Programming in Tcl and Tk: Prentice Hall, 630 p.